Joining and Coating of Plasma Electrolytic Oxidated Aluminum Using a Silica Preceramic Polymer

Transportation Geotechnics 42 (2023) 101073

Contents lists available at ScienceDirect

Transportation Geotechnics

journal homepage: www.elsevier.com/locate/trgeo

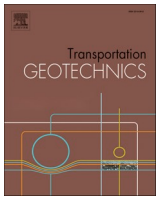

Theoretical modeling of the pre-cutting system performance for the tunnel face stability in very weak rock masses

Vahdat Samandar Ajirlou [a], Masoud Ranjbarnia [a], Pierpaolo Oreste [b,*]

[a] Department of Geotechnical Engineering, Faculty of Civil Engineering, University of Tabriz, Tabriz, Iran
[b] Department of Environmental, Land and Infrastructure Engineering, Politecnico di Torino, Turin, Italy

ARTICLE INFO

Keywords:
Tunnel
pre-cutting shell
convergence confinement method
Squeezing condition

ABSTRACT

By forming continuous pre-lining around the tunnel's perimeter, pre-cutting is a recognized tunneling technique that enables full-face excavation of a tunnel even in unfavorable ground conditions. In this study, a theoretical method is put out to simulate the performance of this kind of pre-support in squeezing conditions. The loading distribution on the pre-cutting shells is determined for this purpose using the LDP of an unsupported tunnel, and the non-linear stiffness of the pre-cutting shell is then determined using the shell theory. The convergence confinement method is used to calculate how much the pre-supported tunnel is deformed. The non-uniform loading distribution also results in the tangential and longitudinal bending moments on the pre-cutting shell. To show the effectiveness of pre-cutting shells in extreme squeezing conditions, several examples are solved. As a result, a few graphs for the preliminary design of a tunnel using this technique are given. The graphs show the overall tunnel displacement for various pre-cutting shells under various geological conditions. The outcomes demonstrate good agreement between FALC 3D results and the ones by the suggested analytical model. A preliminary design can be made using the assessment of the proposed method on the loads on the pre-cutting system.

Introduction

Due to the serious repercussions can have, including the loss of lives, damage to property, and execution delays, tunnel face instability is a major worry under weak ground conditions. When the work is done at a shallow depth, it can also harm surface structures.

There are a variety of methods that can be utilized to limit the tunnel face convergence for secure tunneling and the stability of underground constructions. To be more precise, a low-depth rock mass with good quality would only need a light support system, but a high-depth rock mass with weak quality would need advanced excavation techniques and pre-support systems installed before the main support system could be realized [3,4,6,7,12,16–19,28,36,43–45,47,50,51].

To overcome the instability of the tunnel face and of its perimeter in the safe excavation of soft rocks, various successful preserving and improving methods such as grouting and jet grouting, freezing, pipe arch umbrella, and fiberglass reinforcing elements can be employed according to the severity of geotechnical problems of the ground, cost, and possibility of construction.

A tunnel support method utilized during the initial excavation is the pipe arch umbrella. To reinforce and support the rock mass, a structure must be built above and around the tunnel face. The interaction between the support and the rock mass is the basis for this technique. Numerous research has been conducted to look at different facets of this type of pre-support system's performance. Ranjbarnia et al. [32] investigated the behavior of the arch umbrella supporting system in deep tunnels using the longitudinal deformation profile (LDP) of an unsupported tunnel. The authors suggested an exponential load function on the arch umbrella supporting system by considering each element as a cantilever beam. Oke et al. [22] proposed a semi-analytical model for umbrella-arch systems in squeezing-ground conditions and suggested a second-order equation load distribution on the arch umbrella supporting system using a beam on the elastic foundation theory and the convergence-confinement method. Another attempt was made by Heidari and Tonon [13], who offered a straightforward technique based on the LDP and took into account the hardening effect of jet-grouting umbrella elements. In order to calculate the safety factor of a non-circular tunnel face supported by umbrella elements, Qian et al. [30] combined the strength reduction method with the kinematic approach of the limit analysis.

Bolting is a ground reinforcement method that is experiencing significant growth. This technique provides enduring support to weak rocks

* Corresponding author.

https://doi.org/10.1016/j.trgeo.2023.101073
Received 6 May 2023; Received in revised form 29 July 2023; Accepted 31 July 2023
Available online 12 August 2023

and is highly effective, especially for reinforcing the faces of tunnels. Many authors have conducted studies on the reinforcement of tunnels using fiberglass bolts. Considering a new interpretation of the ground response curve (GRC), Dias [10] used the convergence confinement method (CCM) to calculate the tunnel face deformation reinforced by dowels. Zaheri et al. [46] studied the performance of fiberglass dowels in reducing the deformation of the tunnel face in squeezing grounds analytically using the spherical symmetry hypothesis to obtain the stress distribution ahead of the tunnel face. Oreste [23] introduced an explicit procedure to analyze the dowel's presence in the rock mass. The shear stress was obtained and applied to the dowel-rock interface. Pan and Dias [27] found the safety factor of the tunnel face utilizing both the limit analysis method's kinematic approach and the strength reduction technique.

The design of an umbrella-arch system and longitudinal elements, such as fiberglass bolts, composing single elements (or any other complicated structure) is actually frequently carried out in plain strain conditions to take into account their interaction with the ground. This is done to ensure the stability of the tunnel face. Pre-cutting shell systems are a type of support system that must be built using 3D simulation, either analytically or numerically, to take into account its complicated interaction with the ground. Because of its shell structure, this type of support cannot be designed using plane strain conditions.

The pre-cutting method is a unique construction method that can be employed in soft and severe squeezing conditions, which can be characterize the rock mass at a high depth [41]. It entails placing pre-lining in front of the tunnel face, cutting a nook around the tunnel profile, and pouring shotcrete into a pre-cut shell to create a super-strong roof shell that protects during tunnel driving [29]. However, the pre-cut approach has restrictions related to the size and dimensions that can be achieved as well as the requirement that the cut stays exposed until it is filled with shotcrete. This technique was first introduced in the mining industry in 1950 [39] and used in France in the late seventies, while its application prevailed due to the fact that thirty tunnels were built in Italy and France during the 1980s–1990s. Some recent examples of application of the method allow to verify the technological evolution it has had over the years and its effectiveness in conditions considered difficult [21]. Due to fascinating and beneficial tunneling provided by this technique, such as the full-face excavation and the elimination of the free length during the advancement of the excavation face, its construction technique and application in different environments were studied by numerous researchers (e.g., [20,11]).

Based on the convergence-confinement method, Pelia et al. [29] provided a simple analytical method to design the pre-tunnelling shell. A numerical analysis of the pre-cutting technique, construction sequences, and the effects of various parameters was conducted by Sadaghani and Ebrahimi [34]. For a large-span metro station, Sadaghiani and Dadizadeh [35] presented a novel construction technique called as the Concrete Arc Pre-supporting system. In order to simulate the pre-cutting construction process and examine how the ground responds to the pre-arching in shallow tunnels, Wang et al. [41] tested a geo-mechanical model. The effect of the pre-cutting element's length, thickness, lap length, and sequence of the cutting slots is investigated in this work using a 3D numerical model.

Unlike studying the performance of longitudinal elements, such as umbrella arch systems and fiberglass bolts in stabilizing the tunnel face, there is not a comprehensive study on the performance of shell structures in controlling the convergence of tunnel faces. This paper focuses on the pre-cutting support system as a cylindrical shell and, therefore, employs equations based on the thin shell theory for analytical simulations. Shell structures are also utilized for numerical simulations. In detail, the distribution of the load on this shell is obtained according to the ground squeezing potential and the shell stiffness. Additionally, the flexural moment of the pre-cut shell along the tunnel is also calculated as it may influence its design, and the reduced convergence of the tunnel is obtained at the end.

Most of the previous works about pre-cutting systems have focused on machines, construction methods, and applicable conditions. There is no theoretical investigation nor numerical simulation to illustrate the performance of this system against tunnel face instability and its interaction with the surrounding ground. This study bridges this gap and investigates the role of influencing parameters using the shell theory for the structure of this system and using the principle of the convergence confinement method (the most conventional and rational method for tunneling design).

Problem Definition and General Assumptions

A circular opening is to be excavated with radius r_i in an infinite, isotropic, homogenous weak rock mass subjected to hydrostatic in-situ stresses p_0 [Fig. 1].

Prior to typical excavation, a slot is cut along the periphery of the tunnel, and then is quickly filled with concrete to form a pre-arching shell to provide strong protection (Fig. 2a). Based on rock mass quality and the tunnel depth and size, the shell thickness can be about 7.5–30 cm while its length is from 2 m to 12 m [29]. The overlap in the longitudinal direction between two sequential rings of the shell can be 0.5–1 m to create a tight connection, as shown in Fig. 2b.

The tunnel face advances after the casting of concrete to form the pre-cutting shell. Therefore, the in-situ stresses are redistributed, which leads tunnel face confinement to diminish, and a plastic zone around the tunnel to develop. Although the pre-cutting system is present to confine the tunnel convergence, the surrounding ground is so squeezing that a plastic zone is inevitably developed around the tunnel as a consequence of excavation. That is, the plastic zone has been already developed before the complete activation of the pre-cutting system to apply pressure on the tunnel wall (Fig. 3). In Fig. 3, R and p are respectively the plastic radius and the pressure applied by the pre-cutting shell to the tunnel wall.

To simplify the simulation of the pre-cutting tunneling method, some assumptions are made as follows:

- The pre-cutting shells are elastic;
- The pre-cutting shells are installed with a slight angle with respect to the horizon (Fig. 2). However, its influence is ignored;
- The effect of the sequence of cutting slots on the displacement of these pre-cutting shells is not considered;
- The interaction between the pre-cutting shell and the surrounding rock mass is not considered in the study, which means that the shear stress being created between the ground and the structural element is ignored, and the connection between the shell and the surrounding ground is assumed to be rigid. Consequently, the stress principal direction will not rotate and will remain in radial and tangential directions;

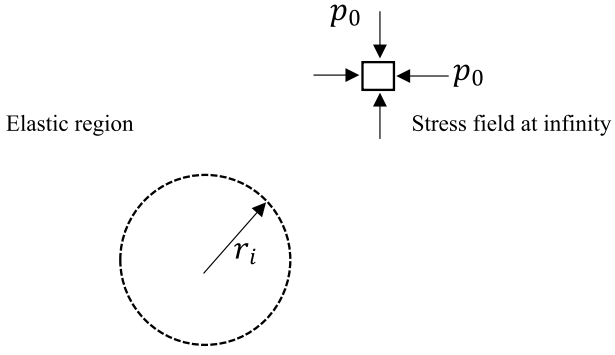

Fig. 1. A circular tunnel is to be excavated in an infinite medium.

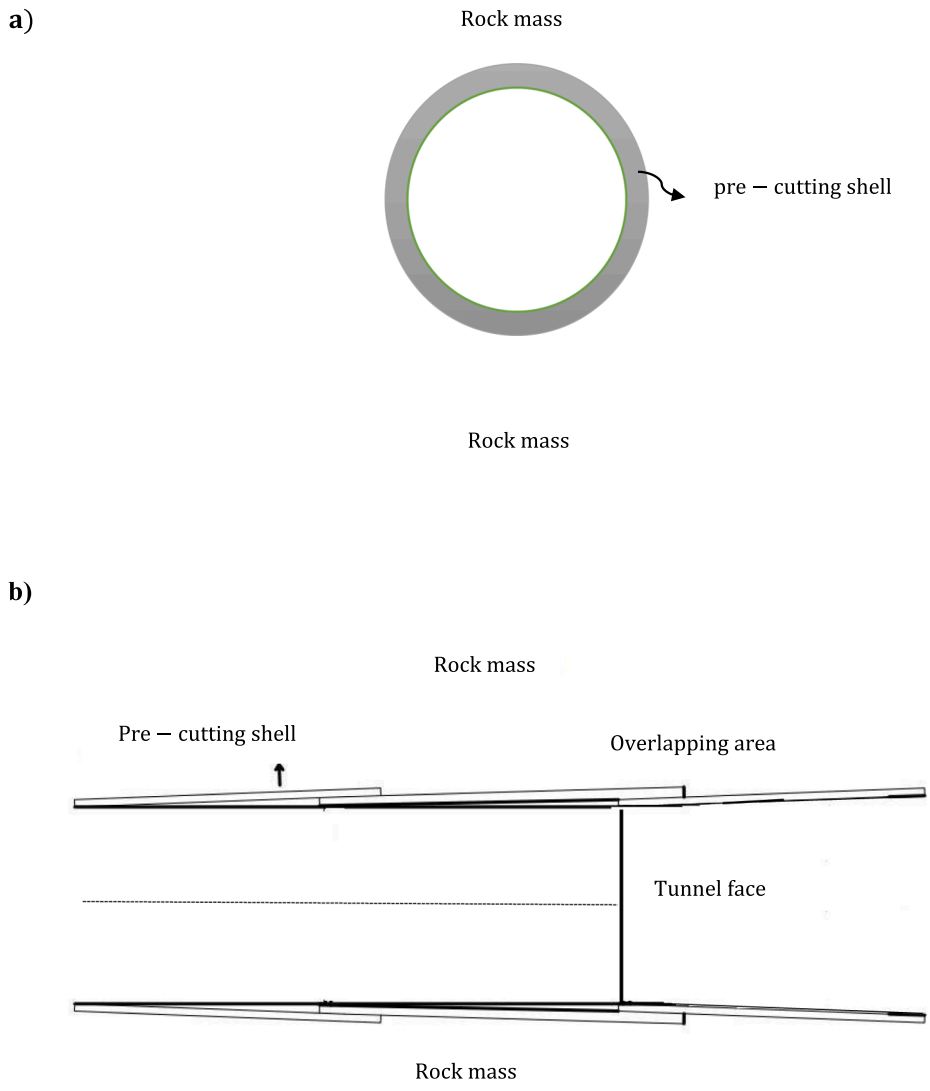

Fig. 2. Schematic view of a pre-cutting tunneling system; a) in the tunnel cross-section, b) in the tunnel longitudinal direction.

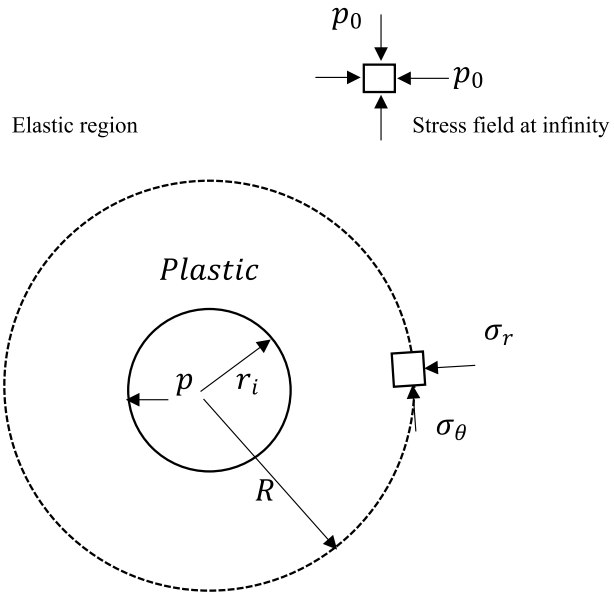

Fig. 3. Development of the plastic zone around the tunnel before pre-cutting activation.

- The deformation of the tunnel is only assumed because of the advancement of the working face. In other words, the time-dependent or creep displacements are neglected;
- The impact of rock weight in the plastic area on the tunnel displacement and support pressures is not considered to retain axisymmetric conditions.

Theoretical simulation

Here, the first pre-cutting shell among the sequence of shells is simulated because it is the critical shell. That is, the beginning of the first shell is free whereas both ends of other shells along the tunnel are supported by an overlap length.

The loading process of a single pre-cutting shell is depicted in Fig. 4, which only shows the deformation and loading process of the crown of the tunnel. The behavior of the pre-cutting shell element in the entrance section of the tunnel, i.e., point (A), in the weak ground is simulated in this study (Fig. 4a). As the tunnel excavation advances, the points *A* and *B* on the tunnel wall are more loaded in every stage of the excavation until the tunnel face reaches far distances (Fig. 4b, c, d). As much length of the pre-cutting shell is loaded in the sequence of excavations, the stiffness of the cylinder shell might decline, which indicates that the support characteristic curve (SCC) might be non-linear (Fig. 4d).

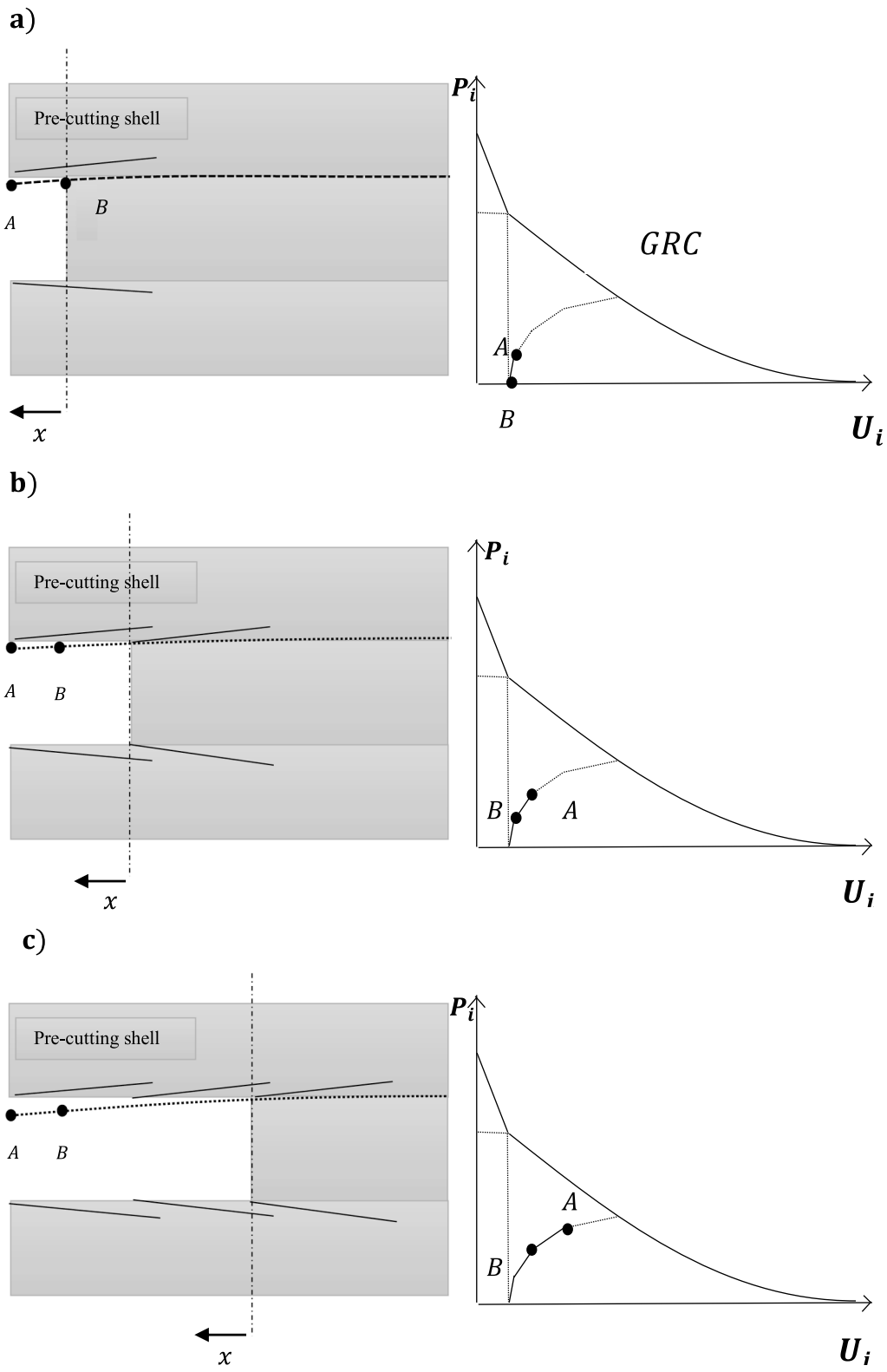

Fig. 4. The loading process of pre-cutting shells in the foregoing excavation stages.

The stiffness of a precutting shell element

A comprehensive examination of the equations necessary for determining the support characteristic curve of a pre-cutting shell element is presented in this section. The support characteristic curve has been obtained for such a continuous support system but in the plain strain condition; however, this section presents a formula in the three-dimensional condition, i.e., it takes the longitudinal direction along the tunnel axis into consideration.

Vlachopoulous and Diederichs [40] asserted that the LDP of a circular tunnel being subjected to the hydrostatic stress (i.e., axisymmetric condition) could be obtained by:

$$U(x) = u\left(1 - \left(1 - \frac{1}{3}exp\left(-0.15\frac{R}{r_i}\right)exp\left(-1.5\frac{x}{R}\right)\right)\right) \; for\; x \geq 0 \quad (1)$$

where u and R are the ultimate deformation and the elastic–plastic boundary radius of an unsupported tunnel, respectively. R can be calculated by equations presented in standard analytical approaches explained in Section 3.3. The variables r_i and x are respectively the tunnel radius and the distance of a desired section from the tunnel face. The longitudinal deformation profile (LDP) of a supported tunnel (by a continuous system such as shotcrete) is similar to an unsupported tunnel [13]. As a result, the modified LDP of the supported tunnels can be found by Eq. (2)

$$U_{sup}(x) = (C_0 \times u)\left(1 - \left(1 - \frac{1}{3}exp\left(-0.15\frac{(C_1 \times R)}{r_i}\right)exp\left(-1.5\frac{x}{(C_1 \times R)}\right)\right)\right)$$

$$for\; x \geq 0 \quad (2)$$

where the parameters C_0 and C_1 are the reduction coefficients that can be obtained from Eq. (3) and Eq. (4) [13]. (SEE: Fig. 5.)

$$C_0 = \frac{U_{ult-sup}}{u} \quad (3)$$

$$\varphi = \frac{U_{sup}(x)}{U(x)} = 0.55 + 0.45C_0 - 0.42(1 - C_0)^3 \quad (4)$$

where $U_{ult-sup}$ and φ are the ultimate convergence of the tunnel with supports and the ratio of the LDP of supported tunnels and that of unsupported ones.

Due to axisymmetric conditions in any cross-section of the tunnel (the circular tunnel under hydrostatic stress conditions) (See Fig. 5), the theory of thin shells can be used to study the performance of pre-cutting shells in a weak rock mass [37].

Therefore, the load distribution on the shell can be calculated according to Timoshenko and Woinowsky-Krieger [37] because the longitudinal displacement of the shell is overlooked and the radius of the tunnel will remain constant when the shell elements are subjected to load.

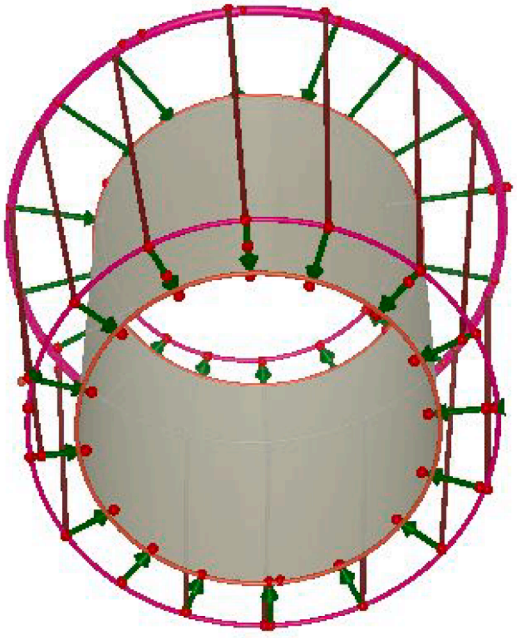

Fig. 5. Schematic of axisymmetric load distribution on a pre-cutting shell.

$$p(x) = -D\frac{d^4(U_{sup}(x))}{dx^4} \quad (5)$$

in which

$$D = \frac{E_c t_{pre-cut}{}^3}{12(1 - \vartheta^2)}$$

where $t_{pre-cut}$ is the shell thickness, and E_c and ϑ are the Elastic Modulus and passion's ratio of the shell, respectively. Replacing Eq. (2) into Eq. (5) gives

$$p(x) = C_2 \exp(1.5\frac{x}{R}) \quad (6)$$

where the parameter C_2 is a combination of C_0 and C_1.

As noticed in Eq. (6), the trend of the radial displacement of the pre-cutting shell is transformed into the radial load distribution. In this regard, Fig. 6 shows the load distribution on a single pre-cutting shell when the tunnel face reaches the beginning point of the subsequent element.

The analytical solution presented in this study is derived from the basic assumption that the longitudinal deformation profile of an unsupported tunnel is used to obtain the loading distribution on the pre-cutting shells. This is because the problems in the vicinity of a tunnel face are three-dimensional and cannot be solved by plane assumption because the convergence of tunnel sections is different from each other, depending on the distance to the tunnel face. The LDP is a tool that makes it possible to obtain the convergence of any tunnel section close to the tunnel face. That is, LDP gives tunnel convergence in the third dimension.

As this paper aims to present a three-dimensional solution based on convergences (and convergence confinement by a pre-cutting system) along the tunnel axis, this approximation is used in developing the analytical solution. Furthermore, the coupling of the ground response curve (GRC) and the LDP gives an exponential relationship between the internal pressures acting on the tunnel wall in different sections along the tunnel axis [8].

In Fig. 6, l_s indicates the length of a single pre-cutting shell, l_o is the overlapping length of two adjacent pre-cutting shells, and l_δ is the distance of the ending point of the overlapping zone from the point on the subsequent shell, which has not been deformed due to excavation and creates a fixed point, i.e., l_δ from the overlapping zone (Figs. 6 and 7). The ground at l_δ from the ending point of the overlapping zone is not impacted by the excavation. This is because the abrupt growth of the thickness of pre-support elements accompanied by tunnel face effect causes the appearance of the point, l_δ from the ending point of the overlapping zone, and at this point, the radial displacements of the transverse sections are significantly lower than those of the adjacent sections [Oreste, [24]]. So, there is no pressure being exerted on the pre-cutting shell element, resulting in no deformation of the supported tunnel. Oreste [24] obtained this value with measuring and performing numerous back-analyses as

$$l_\delta = 0.5\; m\; to\; 0.8\; m \quad (7)$$

The more pre-cutting shell thickness, the more l_δ. That is, it is 0.5 and 0.8 m, respectively, for 30 and 40-cm thicknesses.

Referring to Fig. 6, the tunnel face is located at l_s where the load is not zero, but the cantilever support is located at $l_s + l_o + l_\delta$ (i.e., behind the tunnel face, which is not excavated yet) where the load is zero.

On the other hand, when the tunnel excavation advances and the face reaches sufficiently further distances, the loading on the first pre-cutting shell increases due to the diminished tunnel face confinement and may have almost the load distribution as shown in Fig. 8. However, there is no need to study this case because the non-uniform loading of Fig. 6 produces greater bending moments along the element than the loading of Fig. 8. Obviously, the triangular distribution is different from

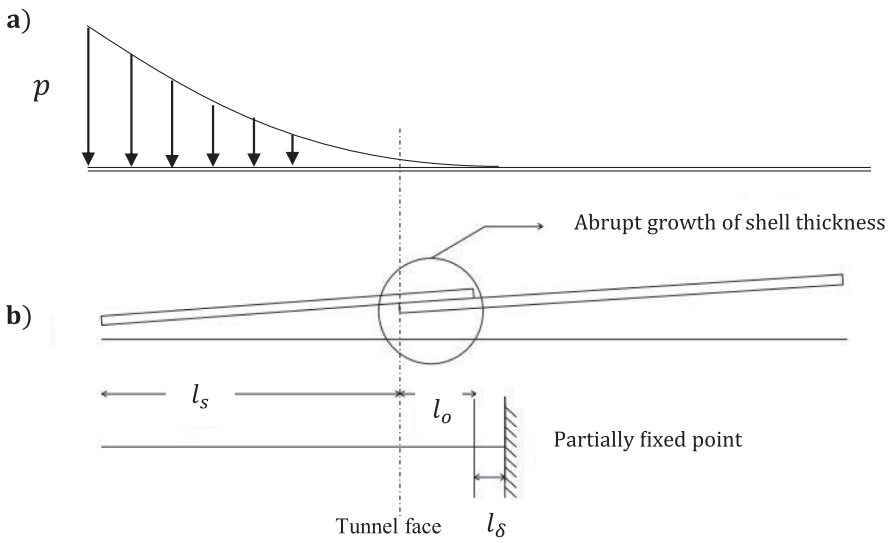

Fig. 6. A) the load distribution acting on a single pre-cutting shell when the tunnel face is at the beginning of the subsequent element; b) consecutive pre-cutting shells and the developed fixed point on the subsequent element.

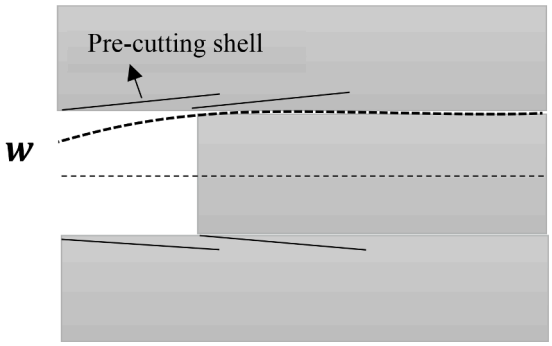

Fig. 7. The deformation of the first pre-cutting shell (w) when the next pre-cutting shell is installed.

the exponential one, and these distributions cannot be replaced with each other. However, the triangular distribution was assumed here so as to it results in a slightly greater equivalent load than the exponential distribution. Therefore, the triangular load distribution causes a slightly greater deformation (and the bending moment on the pre-cutting system) along the tunnel axis. This approximation does not calculate the deformation very exactly, but it provides a convenient way to develop analytical equations.

Therefore, the first shell is studied with a triangular loading. As the shell displacement and the deformed angle are almost negligible at the end of l_δ, the cantilever support is assumed for the boundary condition (Fig. 9). As the load distribution is considered a triangular distribution rather than a exponential distribution, for simplicity:

Then, the load distribution on a single pre-cutting shell is:

$$p(x^{'}) = p - (px^{'}/l) \tag{8}$$

where p is the load magnitude in the entrance section of the tunnel, and l is the total length of the shell obtained by

$$l = l_s + l_o + l_\delta \tag{9}$$

The mechanical response equations for circular shells based on the thin shell theory are presented in Appendix A. This section explains and examines the primary equations used to calculate the longitudinal radial displacements, w (see Fig. 9).

Appendix A shows that the radial displacement of the pre-cutting shell is:

$$w = e^{-\beta x^{''}}\left(\frac{(\sin\beta l)p}{e^{-\beta l}\beta l k_c}\cos\beta x^{''} - \frac{(\cos\beta l)p}{e^{-\beta l}\beta l k_c}\sin\beta x^{''}\right) + \frac{p - (px^{''}/l)}{k_c} \tag{10}$$

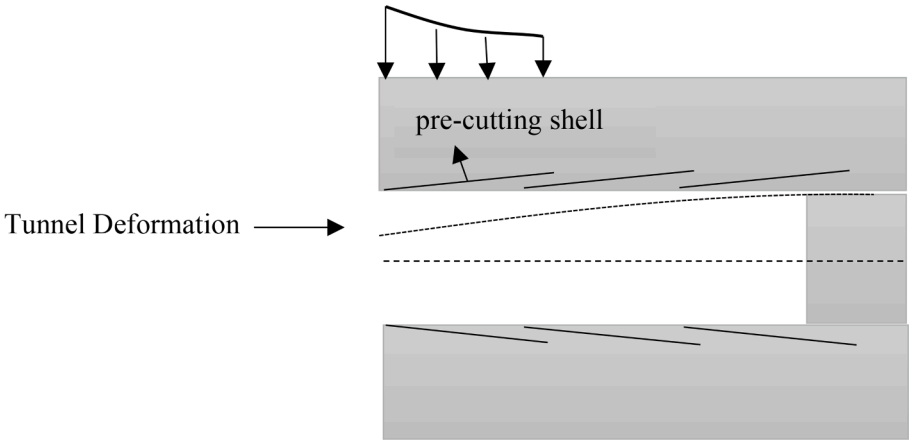

Fig. 8. Load distribution on the first pre-cutting shell when the tunnel face is far from the first element.

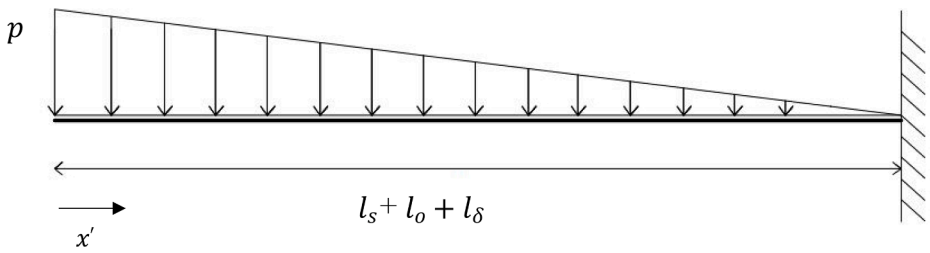

Fig. 9. The simplified distribution of loading on a single pre-cutting shell.

$$M_{x'} = -D\frac{d^2w}{dx'^2} = -D(\beta^2 e^{-\beta x'}\left(\frac{(\sin\beta l)p}{e^{-\beta l}\beta l k_c}\cos\beta x'' - \frac{(\cos\beta l)p}{e^{-\beta l}\beta l k_c}\sin\beta x''\right) + 2\beta e^{-\beta x'}(\frac{(\sin\beta l)p}{e^{-\beta l}lk_c}\sin\beta x'' + \frac{(\cos\beta l)p}{e^{-\beta l}lk_c}\cos\beta x'') + e^{-\beta x'}(\frac{(\cos\beta l)p}{e^{-\beta l}lk_c}\sin\beta x'' - \frac{(\sin\beta l)p}{e^{-\beta l}lk_c}\cos\beta x'') \quad (16)$$

Therefore, the total stiffness of the pre-cutting shell at any point can be computed with the following equation:

$$K_t = \frac{p}{w} \quad (11)$$

Replacing Eq. (10) with Eq. (11) leads to

$$K_t = [\frac{k_c(1-\frac{1}{l}x'')}{\frac{(\sin\beta l)e^{-\beta x''}\cos\beta x'' - (\cos\beta l)e^{-\beta x''}\sin\beta x''}{e^{-\beta l}\beta l} - \frac{1}{l}x'' + 1}] \quad (12)$$

As l is not constant in each step of excavation, it is superseded by the variable x' in Eq. (10), which is depicted in Fig. 10.

Maximum support pressure by a shell element

The primary equations for calculating the maximum tangential stress, $\sigma_{\theta t}$, and maximum pressure exerted on shells are presented and discussed in this section, as shown in Fig. B.1. In Appendix B, the equations for assessing the structural behavior of shells are provided based on the general equation of the radial displacement (Eq. (10)).

Appendix B shows that the total tangential stress exerted on the pre-cutting shell is:

$$\sigma_{\theta t} = \Delta\sigma_\theta + \sigma_\theta \quad (13)$$

where

$$\Delta\sigma_\theta = 12\vartheta M_{x'}/t_{pre-cut}{}^3(r - \left(r_i - \frac{t_{pre-cut}}{2}\right) \quad (14)$$

$$\sigma_\theta = \frac{E_c r_i\left(1 + \frac{(r_i - t_{pre-cut})^2}{r_i^2}\right)w}{(1+\vartheta)[(1-2\vartheta)r_i^2 + (r_i - t_{pre-cut})^2]} \quad (15)$$

Appendix B shows that the bending moment ($M_{x'}$) is:

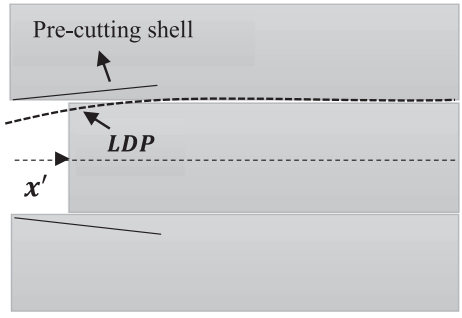

Fig. 10. Superseding the length of the pre-cutting shell with x' while computing the total stiffness of the shell.

To calculate the maximum pressure that can be exerted on a pre-cutting shell with a loading magnitude p in the entrance section, the total tangential stress from Eq. (13) should be equalized to σ_c (the uniaxial compression strength of the shotcrete). For example, the maximum pressure (p_{max}) that can be exerted on a shell (with the thickness of t_c) under constant load p can be obtained by (Fig. 11)[25]:

$$\sigma_{\theta max} = \sigma_c = \frac{2E_c r_i p_{max}}{(1+\vartheta)[(1-2\vartheta)r_i{}^2 + (r_i - t_c{}^3)^2]k_c} \quad (17)$$

$$p_{max} = \frac{\sigma_c\left(1 - \frac{(r_i - t_c{}^3)^2}{r_i{}^2}\right)}{2} \quad (18)$$

In this case, the deflection of any point on the shell in the longitudinal direction can be calculated by [24]:

$$w = \frac{1}{2\beta^3 D}\left(M_0\beta e^{-\beta x}(\cos\beta x - \sin\beta x) - T_0 e^{-\beta x}(\cos\beta x)\right) + \frac{p}{k_c} \quad (19)$$

where

$$M_0 = \frac{2\beta^2 Dp}{k_c} \text{ and } T_0 = \frac{4\beta^3 Dp}{k_c}$$

As shown in Fig. 11, a semi-infinite cylindrical pipe is subjected to the moment M_0 and the shear force T_0 at $x = 0$.

Even though by twice deriving Eq. (19) and by substituting the expression obtained in Eq. (16), the bending moment can be calculated in the longitudinal direction, and its value will be zero [24].

The bending moment caused by the rectangular load distribution is:

$$M_x = e^{-\beta x}\left(M_0(\cos\beta x) + (M_0 + \frac{T_0}{\beta})(\sin\beta x)\right) \quad (20)$$

The Ground Response Curve

In the initial stages of designing the tunnel support, the convergence-confinement method is commonly used as an analytical-visual approach for estimating the necessary support [14]. To implement this method, it is necessary to create the ground reaction curve, which takes into account factors such as the tunnel's diameter, the rock mass's geomechanical properties, and in-situ stresses. More specifically, the GRC of a tunnel can be obtained by standard analytical approaches found elsewhere [1,2,9,26,31,33,42,48,49]. However, any chosen approach should be modified and rewritten according to the elastic-perfectly plastic stress and strain law because it is appropriate for weak rock masses, in which the Geological Strength Index (GSI) is lower than 30 [15].

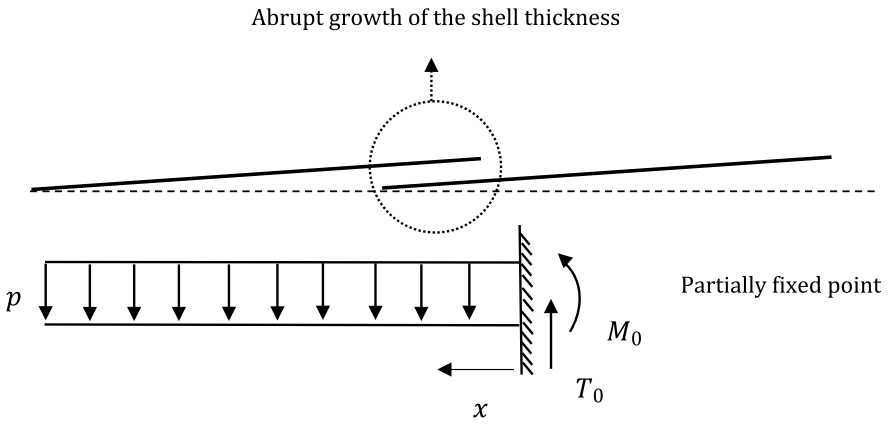

Fig. 11. Static configuration of a shell exposed to a bending moment $\mathbf{M}_0$ and a transverse section shear force..$\mathbf{T}_0$

It is noteworthy that the installation of a pre-support prior to excavation is necessary for tunneling in very severe squeezing conditions, i.e., very weak rock mass at a great depth [16].

Numerical simulation

The problem is simulated using a three-dimensional finite difference code, i.e., FLAC^{3D}. The dimensions of the model subjected to hydrostatic stresses are considered 50 m for the width (x) and the height (z), and 80 m for the length along the tunnel of radius $r_i = 5m$ (y) to eliminate boundary effects on the results. The mesh sizes increase in the radial direction of the tunnel (Fig. 12a), that is, the smallest elements are used near the tunnel boundary.

The horizontal and vertical displacements of the model base as well as the horizontal displacement along the lateral sides are fixed to implement displacement boundary conditions. For the stress boundary of the numerical model, a uniform hydrostatic pressure is applied to the model. It should be noted that the stress variation with depth is not considered since the tunnel is located at a great depth.

The following section discusses the ground characteristic, which is considered a linear elastic-perfectly plastic material with the Hoek-Brown failure criterion and a null dilatancy angle.

Before tunneling, a thin pre-cutting shell is gradually excavated to the length of 3 m around the boundary of the assumed tunnel ahead of the excavation face. Then, the shell elements with a linear elastic material (concrete) are placed in this gap to simulate the pre-cutting (Fig. 12b). In this procedure, the interface conditions between the pre-cutting shell and the surrounding ground are modeled as rigid to coincide with the assumptions of the presented theoretical simulation. Therefore, there is no need to assign the normal stiffness (K_n) and the shear stiffness (K_s) of the ground-shotcrete interface.

Thereafter, the full-face excavation of the tunnel is modeled by gradually removing the ground. The next pre-cutting shell in the overlapping length (as 0.5 m) is modeled by different IDs (numbers allocated to the different shells) for the next shell, i.e., no interface is considered between the two shells to have a rigid connection (Fig. 12c).

To monitor the behavior of the pre-cutting system, ground settlement is measured at the critical point, as shown in Fig. 12c.

Examples

Comparison of the proposed method's predictions with those of other approaches

This paper mainly aims to find the stiffness of the pre-cutting system, which has been schematically shown as SCC in Fig. 4. Section 3.1, as the main part of the paper, provides such a solution. As can be observed in Fig. 4, however, it is required to calculate the GRC to find the tunnel convergence using conventional methods (such as Brown et al. [5] or Park et al. [26]), which consider the rock mass failure criterion and many other details of rock mass characteristics. This is explained in Section 3.3 concisely with no more detail. Therefore, the consideration of the Hoek-Brown failure criterion and the other rock mass properties were hidden in this manuscript.

As a well-established fact, the predictions of a theoretical method should be evaluated to explore its accuracy and efficiency. In this regard, the results of analytical approaches can be verified with those of physical models or with the measured data of a practical project. In the absence of such data, however, the predictions of the suggested method are just compared with those of numerical simulation. Furthermore, the efficiency of the precutting support system with the proposed method is compared with that of an arch umbrella system as it might be considered a lower limit of the pre-cutting system to some extent.

Here, some examples are solved to show the efficiency of the pre-cutting system in confining displacements by the presented theoretical model and by FLAC ^{3D}.

According to Hoek and Marinos [16], the degree of squeezing conditions is identified by $\frac{\sigma_{cm}}{p_0}$, i.e., the ratio of uniaxial compressive strength of rock mass to the maximum in-situ stress. That is, the severe squeezing and the extreme squeezing conditions are identified as class D (in which $\frac{\sigma_{cm}}{p_0}$ is between 0.15 and 0.2) and class E (in which $\frac{\sigma_{cm}}{p_0}$ is less than 0.15), respectively. The installation of a pre-support is necessary for tunneling in these classes [16].

The application example involves a circular tunnel of radius $r_i = 5m$ excavated in a ground with uniform stress p_0. The rock is considered to be intact with a compressive strength of $\sigma_{ci} = 10$MPa, while the rock mass is assumed to be characterized by Hoek-Brown parameters $GSI = 20$, $D = 0$, $m_i = 10$, $m_b = 0.5743$, $s = 0.00013$, and $a = 0.5$ (see [15]). The characteristics of the rock mass's deformability are assumed to be defined by specific parameters $\gamma = 26\text{KN}/m^3$ and $\vartheta = 0.3$, with a null dilation angle. It should be noted that the value of the in-situ stress can be found through $\frac{\sigma_{cm}}{p_0}$ because the uniaxial compressive strength of rock mass (σ_{cm}) can be determined through unconfined compressive strength, the GSI, and the constant m_i [16].

The support system for the tunnel involves a concrete shell, which is assumed to have a Young Modulus of $E_c = 10$GPa and $\vartheta = 0.3$. The mechanical properties of rock masses and tunnels in classes D and E are available in Table 1.

In Table 1, the various categories of weak rock masses are thoroughly examined in relation to distinct pre-cut shell elements. The proposed methodology was used to calculate the tunnel displacements for a circular tunnel excavated at various depths in weak rock masses (i.e., GSI = 20). Specifically, three kinds of pre-cut shell elements were utilized in

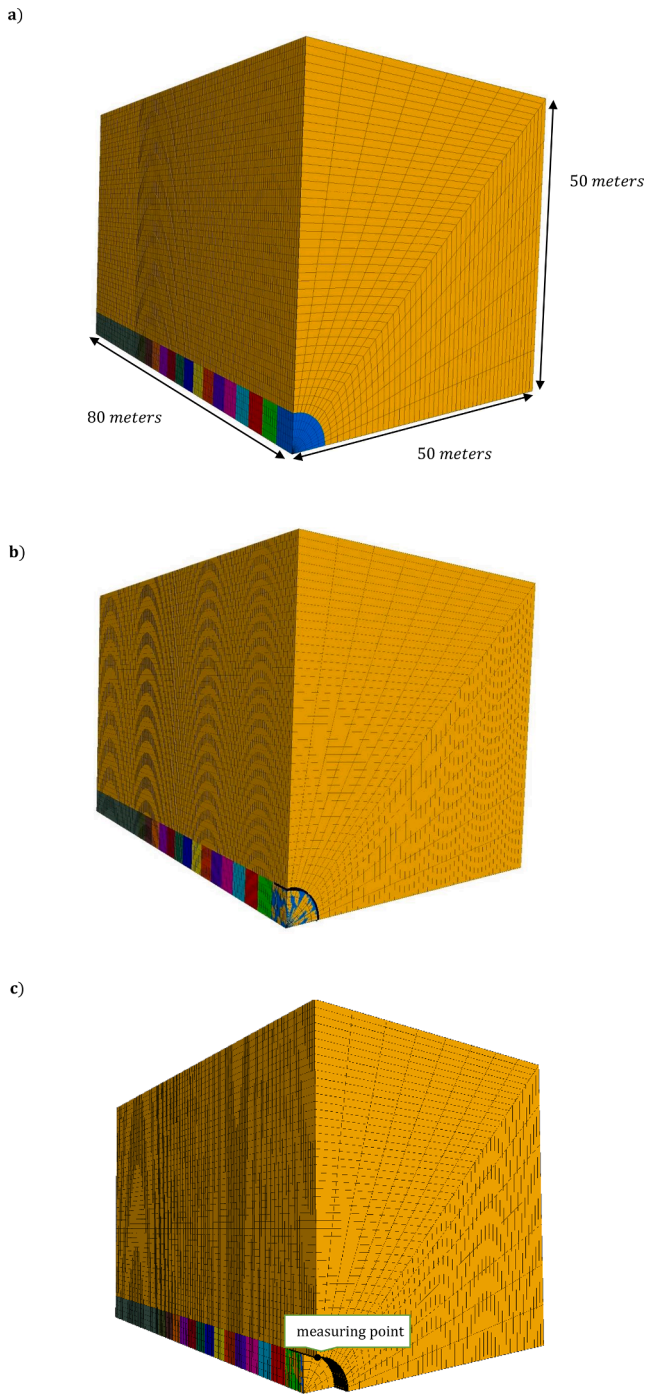

Fig. 12. The view of the 3D numerical model pre-cutting shell. a) Dimensions of the model; b) installation of the pre-cutting shell; c) implementing the overlapping zone and the next pre-cutting shell.

the calculations, resulting in obtaining the LDP of supported tunnels. Consequently, the pre-cutting system can effectively reduce tunnel convergence, as observed above. A good agreement can also be seen between the results of different approaches.

In instances where the rock masses are extremely weak and at significant depths, where the ratio of unconfined compressive strength to the in-situ stress is less than 0.10, unsupported tunnels are inherently unstable. Therefore, it is not feasible to compute the displacements of tunnel walls utilizing FLAC^{3D} software in such scenarios.

Even though different pre-cutting shell thicknesses can be used in the construction of underground structures, it is reasonable to use pre-cutting shell thicknesses in the range of 0.2 m-0.4 for deep tunnels.

Next, the efficiency of pre-cutting shells in highly squeezed conditions is compared with that of the arch umbrella system by considering the minimum distance between umbrella elements. The diameter of umbrella elements is assumed to be the same as the thickness of the pre-cutting shells. For comparison, the length of these two systems is also considered identical as 4 m. The input data (Table 2) are from Ranjbarnia et al. [32] for the assessment of the efficiency of arch umbrella elements in deep tunnels by the theoretical approach.

As can be observed in Table 2, the maximum deformations supported by the arch umbrella system are about 5.42 and 7.29 cm, while those of the pre-cutting method are less than 1.3 and 1.6 cm, when $\frac{\sigma_{cm}}{p_0}$ are 0.15 and 0.13, respectively. The aim is to show that the proposed method predicts remarkably smaller convergence by the pre-cutting support system than the arch umbrella system.

Furthermore, if the spacing of the outer surface of the umbrella elements decreases from $d_t = 0.5$ m to 0.05 m, the convergence will be reduced to 1.9 cm from 5.42 cm and 2.38 cm from 7.29 cm. These values (1.9 cm and 2.38 cm) are comparable to those of employing the pre-cutting system (in which the convergences are 1.3 and 1.6 cm). It indicates that if the spacing between the arch umbrella elements becomes very small, that system may approximately act as a pre-cutting shell system in the periphery of the tunnel.

The proposed method is verified indirectly by comparing its results with the arch umbrella system and with numerical modeling by FLAC^{3D}, but the proposed method seems to give the results with good accuracy.

The influence of the parameters associated with the pre-cutting system stiffness

In this section, the performance of the precutting system at different conditions is evaluated using the proposed analytical approach. The stiffness of each pre-cutting shell is sized by its thickness and elastic properties (See Eq. (A.4).). As observed in Fig. 13, the transverse-section stiffness of the tunnel increases significantly with the thickness of the shells, and the short time convergence of the tunnel in different squeezing conditions is markedly reduced by increasing pre-cutting shells stiffness. Therefore, the pre-cutting technique is efficient in tunnels of squeezing conditions where it is necessary to control the unstable rock mass. The performance of distinct types of pre-cutting shell elements in diverse weak ground conditions appears to exhibit comparable trends due to the simplifications made while creating the analytical mode. Fig. 14 exhibits the corresponding LDP of the supported tunnel with pre-cutting shell elements obtained by calculations performed by the proposed analytical approach for two types of pre-cutting shell elements in the same geometrical configuration.

Furthermore, the thickness of the pre-support directly influences the pre-cutting stiffness magnitude and, therefore, can decline dramatically the convergence of the tunnel wall. As shown in Eq. (12), the longitudinal stiffness of the pre-cutting shell depends on the transverse stiffness of the tunnel cross-section. The foregoing formulation was used to evaluate the pre-cutting shell system for different mechanical and geometrical configurations. In Fig. 15, the effects of the transverse stiffness are investigated by considering three different scenarios to depict the reduced deformations of the tunnel wall (as the representative of tunnel stability) in terms of using typical values of pre-cutting thickness in the rock mass with GSI = 20 (as the representative of a weak ground) at conventional depths. It can be used for the fast-preliminary design of pre-tunneling shells provided that the concrete does not fail due to developed stresses. This issue is discussed in Section 5.3.

Table 1
The properties of pre-cutting shells and output results obtained by simulation based on CCM and FLAC^{3D} models.

$\frac{\sigma_{cm}}{p_0}$	GSI	SqueezingClass	$U_{un-supported} \times 10^{-2}(m)$	$t_{pre-cutting}$	$U_{Analytical} \times 10^{-2}(m)$	$U_{Flac} \times 10^{-2}(m)$
0.15	20	D	10.24	0.3	1.529	1. 518
				0.35	1.41	1. 41
				0.4	1.297	1. 299
0.13	20	E	13.5	0.3	1.776	1. 77
				0.35	1.65	1. 63
				0.4	1.555	1. 509
0.11	20	E	25.6	0.3	2.166	2. 145
				0.35	2.057	1. 965
				0.4	1.87	1. 815

Table 2
The comparisons between predictions of the umbrella element system and the pre-cutting tunneling system.

$\frac{\sigma_{cm}}{p_0}$	class	$t_{pre-cutting}(cm)$	$D(m)$	$t(cm)$	$U_{un-supported}(cm)$	$U_{umb}(cm)$	$U_{pre-cutting}(cm)$
0.15	D	40	0.4	2	10.24	5.42	1.297
0.13	E	40	0.4	2	13.5	7.29	1.555

$d_t = 0.5m$ is the distance of the outer surface of two umbrella elements.
*t is the thickness of arch umbrella elements.
*D is the diameter of arch umbrella elements. 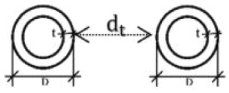

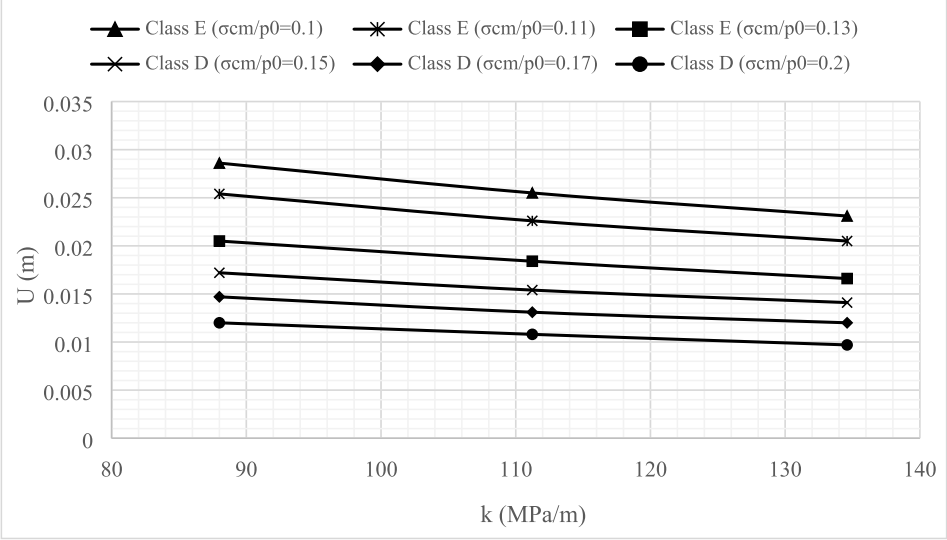

Fig. 13. The influence of pre-cutting stiffness ($\mathbf{k_c}$) on the confinement of tunnel wall convergence.

Structural Design of the pre-cutting system

The preliminary design of the shotcrete layer in circular tunnels under a hydrostatic stress field can be obtained by the equation proposed by Hoek and Brown [14]. This equation is appropriate for the plane strain condition (e.g., in the section located far from the tunnel face under uniform load), and the tangential stress acting on the shell is the only main factor.

However, the load on a pre-cutting shell is not uniform along the tunnel, and a bending moment is effective in addition to the tangential stress.

To find the point at which the maximum bending moment is along the pre-cutting shell, the shear force should be zero. That is:

$$T_{x'} = \frac{dM}{dx'} = 0 \ \ then \ \ x'_{Mmax} = \frac{arctg\frac{\sin\beta l - cos\beta l}{\sin\beta l + cos\beta l}}{\beta} - l_\delta \tag{21}$$

Thus, the maximum bending moment can be obtained by replacing Eq. (21) with Eq. (16), and the stress created by the maximum bending moment can be calculated using Eq. (22)

$$\sigma_{\theta max} = 6\vartheta M_{x'max}/{t_{pre-cut}}^3 \tag{22}$$

As a result, the stress created by the maximum bending moment must be added to the tangential stress.

A study was developed to understand whether or not the developed stress from the maximum bending moment is considerable. To be more specific, this section aims to show whether or not the influence of the bending moment is significant in the total amount of stress considered in the design of shells. Accordingly, attempts are implemented to find if the structural design of the pre-cutting shell (i.e., the required thickness of the shells) can be obtained simply using the equation of Hoek and Brown [14], or if it is necessary to consider the effect of the bending moment as well.

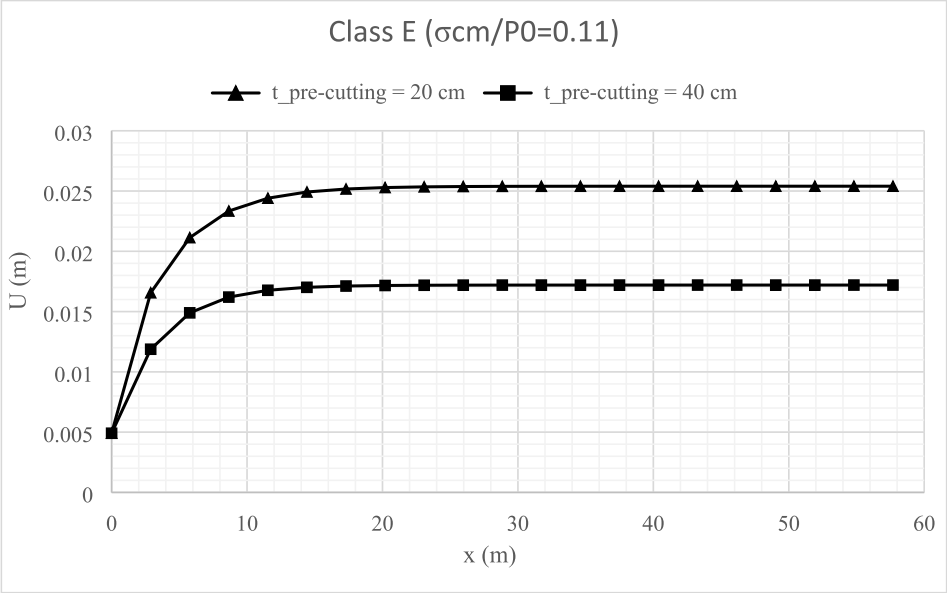

Fig. 14. The longitudinal deformation profile (**LDP**) of the supported tunnel by the pre-cutting shell.

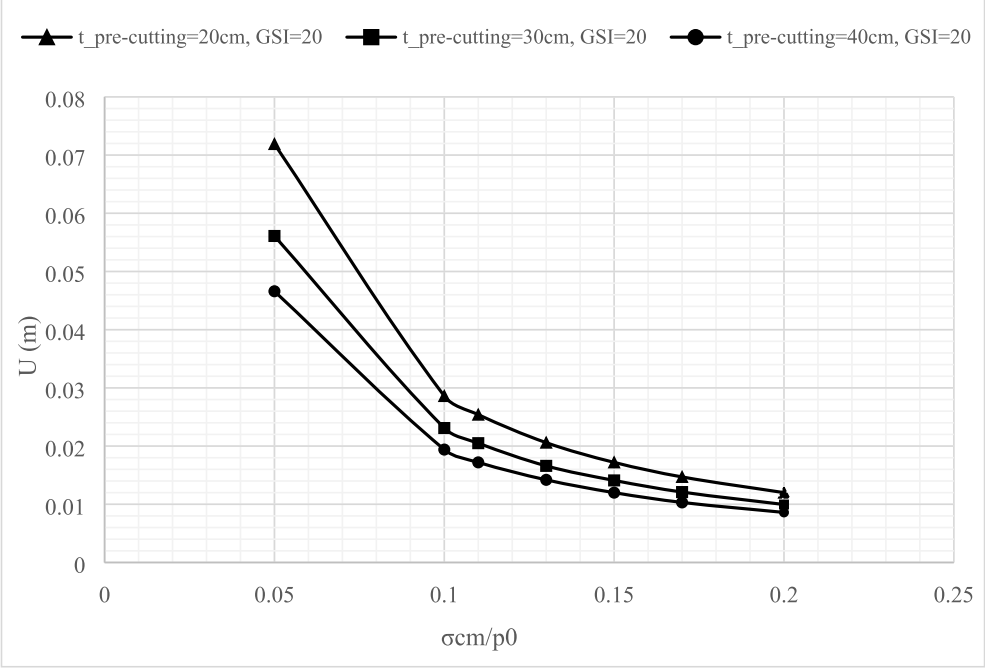

Fig. 15. The performance of the pre-cutting shell in various squeezing conditions.

Table 3
The comparison of circumferential stress created by the bending moment in the proposed approach with the circumferential stress proposed by the classic approach.

$\frac{\sigma_{cm}}{p_0}$	*GSI*	*class*	$t(m)$	$\sigma_{\theta Mmax}(MPa)$	$\sigma_{\theta classic}(MPa)$	$\frac{\sigma_{\theta Mmax}}{\sigma_{\theta classic}} \times 10^{-2}$
0.15	20	D	0.3	3.33	16.438	20
0.13	20	E	0.35	3.654	21.437	17
0.11	20	E	0.4	4.052	27.983	14. 5

Table 3 gives the ratio of the stress created by the maximum bending moment to the circumferential stress calculated according to Hoek-Brown [14]. As observed, the developed stress from the bending moment is remarkable, and therefore, it is not possible to define the thickness of the pre-cutting shell only by the equation of Hoek-Brown [14].

Conclusions

By using the pre-cutting tunneling technique, a theoretical model was shown to analyze the behavior of the ground and pre-lining, and the model results were strengthened by carrying out numerical calculations.

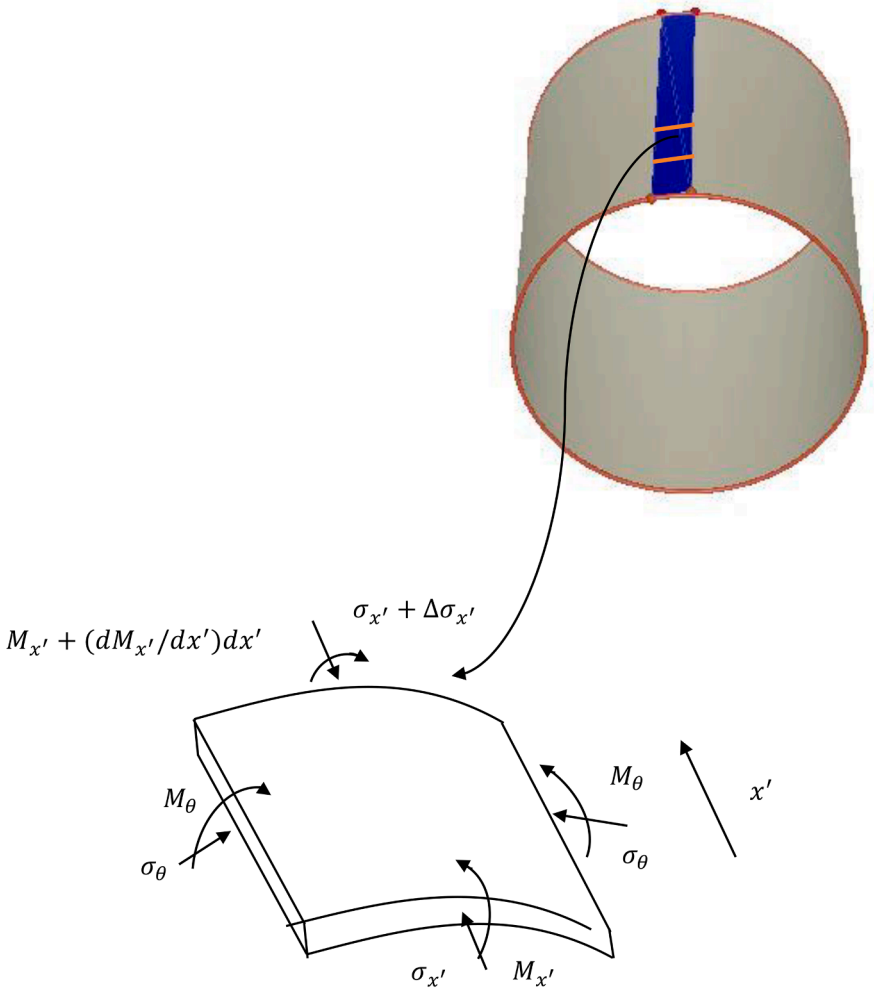

Fig. B1. An infinitesimal element of the shell in the longitudinal direction.

In severely unstable and squeezing conditions, the analytical technique can be employed for the quick and preliminary design of a pre-cutting system. Thus, the findings were displayed in the form of a few graphs that expressed the displacement of the pre-supported tunnel as a function of the ratio of the uniaxial strength of the rock mass to the in-situ stress. Now that more advanced numerical techniques have been developed, these results can be used as the starting point for more accurate modeling.

Furthermore, the full set of equations needed to obtain the support characteristic curve for a pre-cutting shell element is presented in the preceding sections of this paper. The closed-form analytical approach can be easily used to obtain the longitudinal stiffness of shells, which can be used by practitioners as a first-order estimate for the structural design and analysis of the liner.

The sensitive study concludes by demonstrating that the stiffness of pre-cutting shells—specifically, the thickness of the pre-cutting shell—is more effective than the other parameters in regulating tunnel displacements. The analytical equation by [14] that was used for the initial design of the shotcrete layer results in an imprecise assessment of the pre-cutting system requirements as well.

It should be emphasized that the findings drawn above are strictly theoretical in nature and do not account for variables like the actual slot-cutting rate, the schedule for filling, intermittent construction practices, etc. The planned model and the actual building may thus have some specific differences.

CRediT authorship contribution statement

Vahdat Samandar Ajirlou: Methodology, Software, Writing – original draft. **Masoud Ranjbarnia:** Conceptualization, Methodology, Data curation, Writing – original draft, Writing – review & editing, Validation. **Pierpaolo Oreste:** Supervision, Validation, Writing – review & editing.

Declaration of Competing Interest

The authors declare that they have no known competing financial interests or personal relationships that could have appeared to influence the work reported in this paper.

Data availability

No data was used for the research described in the article.

Appendix A. . Elastic solution of a circular shell subjected to a triangular distributed load

The solution presented in this appendix is derived from the formulation of thin elastic shells described in Timoshenko and Woinowsky-Krieger [37]. The main text provides a description of the variables used in this formulation. Fig. 9 illustrates the problem to be solved, which involves a circular shell with a radius of r_i and a length of l (Eq. (9)). The overall deformation of a shell can be determined with Eq. (A.1) [37].

$$w = e^{\beta x'}(C_3\cos\beta x' + C_4\sin\beta x') + e^{-\beta x'}(C_5\cos\beta x' + C_6\sin\beta x') \tag{A.1}$$

As the shell being analyzed is exposed to an external load, an added heterogeneous term, which accounts for the load distribution, is incorporated into Eq. (A.1) to have:

$$w = e^{\beta x''}(C_4\cos\beta x'' + C_5\sin\beta x'') + e^{-\beta x''}(C_6\cos\beta x'' + C_7\sin\beta x'') + \frac{p(x'')}{k_c} \tag{A.2}$$

in which

$\beta^4 = \frac{3(1-\vartheta^2)}{r^2(t_{pre-cut})^2}$, $x'' = x' + l_\delta$, and.where the parameter k_c is the tangential stiffness of a transverse section of the cylindrical shell, depending on the stage of excavation. In the case in which the tunnel face is near a desired section, it is (Timoshenko and Woinowsky-Krieger, [37]):

$$k_c = \frac{E_c t_{pre-cut}}{{r_i}^2} \tag{A.3}$$

However, in the case in which the tunnel face is far from the desired section, it is [24]:

$$k_c = \frac{E_c({r_i}^2 - (r_i - t_{pre-cut})^2)}{r_i(1+\vartheta)[(1-2\vartheta){r_i}^2 + (r_i - t_{pre-cut})^2]} \tag{A.4}$$

The coefficients C_4, C_5, C_6, and C_7 can be calculated through the boundary condition shown in Fig. 9. As the shell thickness is smaller than its radius and length, the shell can be considered infinitely long [37]. Consequently,

- the constants C_4 and C_5 are zero since Saint and Venant's principle can be applied for this simulation [38]. That is, the effect of stress applied to a small part of a long shell will dissipate at farther distances [38], making the first term of Eq. (A.2) negligible.
- the constants C_6 and C_7 can be obtained by the boundary condition of overlapping length that treats as cantilever support. Hence;

$$(w)_{x'=l} = 0 \rightarrow C_6 = \frac{(\sin\beta l)p}{e^{-\beta l}\beta((\sin\beta l)^2 + (\cos\beta l)^2)lk_c} = \frac{(\sin\beta l)p}{e^{-\beta l}\beta l k_c} \tag{A.5}$$

$$\left(\frac{dw}{dx'}\right)_{x'=l} = 0 \rightarrow C_7 = -\frac{(\cos\beta l)p}{e^{-\beta l}\beta((\sin\beta l)^2 + (\cos\beta l)^2)lk_c} = -\frac{(\cos\beta l)p}{e^{-\beta l}\beta l k_c} \tag{A.6}$$

Eq. (A.2) then becomes

$$w = e^{-\beta x''}\left(\frac{(\sin\beta l)p}{e^{-\beta l}\beta l k_c}\cos\beta x'' - \frac{(\cos\beta l)p}{e^{-\beta l}\beta l k_c}\sin\beta x''\right) + \frac{p - (px''/l)}{k_c} \tag{A.7}$$

Appendix B. . Solution of circular elastic shells according to the theory of thin shells

This appendix provides a demonstration of equations for the analysis of shells. If a cylindrical shell is exposed to hydrostatic pressure, i.e., the development of the axisymmetric condition (see Fig. 5), the variation of the bending moment in the tangential direction (M_θ) is null (see Fig. B.1), and the produced tangential stress is found according to Brown et al. [5]:

$$\sigma_\theta = \frac{E_c r_i\left(1 + \frac{(r_i - t_{pre-cut})^2}{r^2}\right)w}{(1+\vartheta)[(1-2\vartheta){r_i}^2 + (r_i - t_{pre-cut})^2]} \tag{B.1}$$

in which r is the generic coordinate (distance from the tunnel axis).

As w is variable, the tangential stress is variable in the longitudinal direction.

The tangential bending moment M_θ is calculated by

$$\begin{aligned} M_\theta &= \int_{r_i - t_{pre-cut}}^{r_i} \sigma_\theta\left(r - \left(r_i - \frac{t_{pre-cut}}{2}\right)\right)dr \\ &= \frac{E_c r_i w}{(1+\vartheta)\left[(1-2\vartheta){r_i}^2 + (r_i - t_{pre-cut})^2\right]}\left(\frac{r_i}{2} + (r_i - t_{pre-cut})^2\left(ln\frac{r_i}{r_i - t_{pre-cut}} - \frac{1}{2}\right) - \left(r_i - \frac{t_{pre-cut}}{2}\right)(r_i - t_{pre-cut})\frac{t_{pre-cut}}{r_i} + t_{pre-cut}\right) \end{aligned} \tag{B.2}$$

On the other hand, the relationship between the bending moment in the longitudinal direction, i.e., $M_{x'}$, and the longitudinal stress $\Delta\sigma_{x'}$ is:

$$M_{x'} = \int_{r_i - t_{pre-cut}}^{r_i} \Delta\sigma_{x'}\left(r - \left(r_i - \frac{t_{pre-cut}}{2}\right)\right)dr \tag{B.3}$$

Thus,

$$\Delta\sigma_{x'} = 12M_{x'}/{t_{pre-cut}}^3\left(r-\left(r_i-\frac{t_{pre-cut}}{2}\right)\right) \tag{B.4}$$

The bending moment can be obtained from the second derivative of Eq. (10):

$$M_{x'} = -D\frac{d^2w}{dx'^2} = -D(\beta^2 e^{-\beta x''}\left(\frac{(\sin\beta l)p}{e^{-\beta l}\beta l k_c}\cos\beta x'' - \frac{(\cos\beta l)p}{e^{-\beta l}\beta l k_c}\sin\beta x''\right) + 2\beta e^{-\beta x''}(\frac{(\sin\beta l)p}{e^{-\beta l}lk_c}\sin\beta x'' + \frac{(\cos\beta l)p}{e^{-\beta l}lk_c}\cos\beta x'') + e^{-\beta x''}(\frac{(\cos\beta l)p}{e^{-\beta l}lk_c}\sin\beta x'' - \frac{(\sin\beta l)p}{e^{-\beta l}lk_c}\cos\beta x'') \tag{B.5}$$

Then, ΔM_θ is produced by Eq. (B.4), which should be added to.M_ϑ

The increase of tangential stress when the tangential displacements are prevented is found by $\Delta\sigma_\theta = \vartheta\Delta\sigma_{x'}$. Therefore,

$$\Delta M_\theta = \int_{r_i-t_{pre-cut}}^{r_i} \vartheta\Delta\sigma_{x'}\left(r-\left(r_i-\frac{t_{pre-cut}}{2}\right)\right)dr = \vartheta M_{x'} \tag{B.6}$$

As a result, the total tangential stress is obtained by

$$\sigma_{\theta t} = \Delta\sigma_\theta + \sigma_\theta \tag{B.7}$$

in which

$$\Delta\sigma_\theta = 12\vartheta M_{x'}/{t_{pre-cut}}^3\left(r-\left(r_i-\frac{t_{pre-cut}}{2}\right)\right) \tag{B.8}$$

In fact, Eq. (B.8) is the result of the variable moment in the longitudinal direction, i.e., $M_{x'}$.

References

[1] Alejano LR, Rodriguez-Dono A, Alonso E, Manín GF. Ground reaction curves for tunnels excavated in different quality rock masses showing several types of post-failure behaviour. Tunn Undergr Space Technol 2009;24(6):689–705. https://doi.org/10.1016/j.tust.2009.07.004.

[2] Alonso E, Alejano LR, Varas F, Fdez-Manin G, Carranza-Torres C. Ground response curves for rock masses exhibiting strain-softening behaviour. Int J Numer Anal Meth Geomech 2003;27(13):1153–85. https://doi.org/10.1002/nag.315.

[3] Antão AN, da Silva MV, Monteiro N, Deusdado N. Upper and lower bounds for three-dimensional undrained stability of shallow tunnels. Transp Geotech 2021;1(27):100491. https://doi.org/10.1016/j.trgeo.2020.100491.

[4] Barla G, Bonini M, Semeraro M. Analysis of the behaviour of a yield-control support system in squeezing rock. Tunn Undergr Space Technol 2011;26(1):146–54. https://doi.org/10.1016/j.tust.2010.08.001.

[5] Brown ET, Bray JW, Ladanyi B, Hoek E. Ground response curves for rock tunnels. J Geotech Eng 1983;109(1):15–39. https://doi.org/10.1061/(ASCE)0733-9410(1983)109:1(15).

[6] Chen RP, Lin XT, Wu HN. An analytical model to predict the limit support pressure on a deep shield tunnel face. Comput Geotech 2019;1(115):103174. https://doi.org/10.1016/j.compgeo.2019.103174.

[7] Chu Z, Wu Z, Liu Q, Liu B. Analytical solutions for deep-buried lined tunnels considering longitudinal discontinuous excavation in rheological rock mass. J Eng Mech 2020;146(6):04020047. https://doi.org/10.1061/(ASCE)EM.1943-7889.0001784.

[8] Chu Z, Wu Z, Liu B, Liu Q. Coupled analytical solutions for deep-buried circular lined tunnels considering tunnel face advancement and soft rock rheology effects. Tunn Undergr Space Technol 2019;1(94):103111. https://doi.org/10.1016/j.tust.2019.103111.

[9] Cui L, Sheng Q, Zheng JJ, Cui Z, Wang A, Shen Q. Regression model for predicting tunnel strain in strain-softening rock mass for underground openings. Int J Rock Mech Min Sci 2019;1(119):81–97. https://doi.org/10.1016/j.ijrmms.2019.04.014.

[10] Dias D. Convergence-confinement approach for designing tunnel face reinforcement by horizontal bolting. Tunn Undergr Space Technol 2011;26(4):517–23. https://doi.org/10.1016/j.tust.2011.03.004.

[11] Eisenstein Z, Ezzeldine O. The effect of tunnelling technology on ground control. Tunn Undergr Space Technol 1992;7(3):273–9. https://doi.org/10.1016/0886-7798(92)90008-6.

[12] Fang Y, Su Y. On the use of the global sensitivity analysis in the reliability-based design: Insights from a tunnel support case. Comput Geotech 2020;1(117):103280. https://doi.org/10.1016/j.compgeo.2019.103280.

[13] Heidari M, Tonon F. Ground reaction curve for tunnels with jet grouting umbrellas considering jet grouting hardening. Int J Rock Mech Min Sci 2015;1(76):200–8. https://doi.org/10.1016/j.ijrmms.2015.03.021.

[14] Hoek E, Brown ET. Empirical strength criterion for rock masses. J Geotech Eng Div 1980;106(9):1013–35. https://doi.org/10.1061/AJGEB6.0001029.

[15] Hoek E, Brown ET. Practical estimates of rock mass strength. Int J Rock Mech Min Sci 1997;34(8):1165–86. https://doi.org/10.1016/S1365-1609(97)80069-X.

[16] Hoek E, Marinos P. Predicting tunnel squeezing problems in weak heterogeneous rock masses. Tunnels Tunnel Int 2000;32(11):45–51.

[17] Hu X, Fang Y, Walton G, He C. Analysis of the behaviour of a novel support system in an anisotropically jointed rock mass. Tunn Undergr Space Technol 2019;1(83):113–34. https://doi.org/10.1016/j.tust.2018.09.028.

[18] Hu XY, He C, Lai XH, Walton G, Xu GW. Study on the interaction between squeezing ground and yielding supports with different yielding materials. Tunn Undergr Space Technol 2020;1(97):103242. https://doi.org/10.1016/j.tust.2019.103242.

[19] Hu X, Gutierrez M. Analytical model for deep tunnel with an adaptive support system in a viscoelastic-burger's rock. Transp Geotech 2022;1(35):100775. https://doi.org/10.1016/j.trgeo.2022.100775.

[20] Johnson EB, Holloway LJ, Kjerbol G. Design of Mt. Baker Ridge Freeway Tunnel in Seattle. In Proceeding, Rapid Excavation and Tunnelling Conference 1983 (Vol. 1, pp. 439-458).

[21] Lunardi G, Agresti S, Basta D. The widening of the "Montedomini" A14 Motorway Tunnel in the presence of traffic. In Proceedings of the ITA-AITES World Tunnel Congress 2016 (WTC 2016), San Francisco, CA, USA, 22–28 April 2016. pp. 1–10.

[22] Oke J, Vlachopoulos N, Diederichs MS. Semi-analytical model for umbrella arch systems employed in squeezing ground conditions. Tunn Undergr Space Technol 2016;1(56):136–56. https://doi.org/10.1016/j.tust.2016.03.006.

[23] Oreste P. Face stabilization of deep tunnels using longitudinal fibreglass dowels. Int J Rock Mech Min Sci 2013;1(58):127–40. https://doi.org/10.1016/j.ijrmms.2012.07.011.

[24] Oreste PP. The importance of longitudinal stress effects on the static conditions of the final lining of a tunnel. Tunnel Undergr Space Technol 2002;17(1):21–32. https://doi.org/10.1016/S0886-7798(01)00069-4.

[25] Oreste PP. Analysis of structural interaction in tunnels using the covergence–confinement approach. Tunnell Undergr Space Technol 2003;18(4):347–63. https://doi.org/10.1016/S0886-7798(03)00004-X.

[26] Park KH, Tontavanich B, Lee JG. A simple procedure for ground response curve of circular tunnel in elastic-strain softening rock masses. Tunn Undergr Space Technol 2008;23(2):151–9. https://doi.org/10.1016/j.tust.2007.03.002.

[27] Pan Q, Dias D. Upper-bound analysis on the face stability of a non-circular tunnel. Tunn Undergr Space Technol 2017;1(62):96–102. https://doi.org/10.1016/j.tust.2016.11.010.

[28] Pandit B, Babu GS. Probabilistic stability assessment of tunnel-support system considering spatial variability in weak rock mass. Comput Geotech 2021;1(137):104242. https://doi.org/10.1016/j.compgeo.2021.104242.

[29] Peila D, Oreste PP, Rabajoli G, Trabucco E. The pretunnel method, a new Italian technology for full-face tunnel excavation: a numerical approach to design. Tunn Undergr Space Technol 1995;10(3):367–74. https://doi.org/10.1016/0886-7798(95)00017-S.

[30] Qian Z, Zou J, Pan Q, Dias D. Safety factor calculations of a tunnel face reinforced with umbrella pipes: A comparison analysis. Eng Struct 2019;15(199):109639. https://doi.org/10.1016/j.engstruct.2019.109639.

[31] Ranjbarnia M, Fahimifar A, Oreste P. Analysis of non-linear strain-softening behaviour around tunnels. Proc Institut Civil Eng-Geotech Eng 2015;168(1):16–30. https://doi.org/10.1680/geng.13.00144.

[32] Ranjbarnia M, Rahimpour N, Oreste P. A simple analytical approach to simulate the arch umbrella supporting system in deep tunnels based on convergence confinement method. Tunn Undergr Space Technol 2018;1(82):39–49. https://doi.org/10.1016/j.tust.2018.07.033.

[33] Ranjbarnia M, Rahimpour N, Oreste P. A new analytical-numerical solution to analyze a circular tunnel using 3D Hoek-Brown failure criterion. Geomech Eng 2020;22(1):11–23. https://doi.org/10.12989/gae.2020.22.1.011.

[34] Sadaghiani MH, Ebrahimi A. Stability analysis of construction sequences of a large underground metro station using Concrete Arc Pre-Supporting System (CAPS). In: Proceedings, 7th Iranian Tunnelling Conference, Tehran, Iran, 2006; pp. 417–426.

[35] Sadaghiani MH, Dadizadeh S. Study on the effect of a new construction method for a large span metro underground station in Tabriz-Iran. Tunn Undergr Space Technol 2010;25(1):63–9. https://doi.org/10.1016/j.tust.2009.08.004.

[36] Song X, Wu HN, Meng FY, Chen RP, Cheng HZ. Soil arching evolution caused by shield tunneling in deep saturated ground. Transp Geotech 2023;1(40):100966. https://doi.org/10.1016/j.trgeo.2023.100966.
[37] Timoshenko S, Woinowsky-Krieger S. Theory of plates and shells. New York: McGraw-hill; 1959.
[38] Timoshenko S, Goodier JN. Theory of Elasticity" McGraw-Hill Book Company. New York: Inc; 1951.
[39] Van Walsum E. Mechanical pre-cutting, a rediscovered tunneling technique. Rock Mech Rock Eng 1991;24(2):65–79. https://doi.org/10.1007/BF01032499.
[40] Vlachopoulos N, Diederichs MS. Improved longitudinal displacement profiles for convergence confinement analysis of deep tunnels. Rock Mech Rock Eng 2009;42:131–46. https://doi.org/10.1007/s00603-009-0176-4.
[41] Wang T, Wang X, Tan Z, Li K, He M. Studies on ground settlement and pre-arching stress of pre-cutting tunnelling method. Tunn Undergr Space Technol 2018;1(82):199–210. https://doi.org/10.1016/j.tust.2018.08.021.
[42] Wang HN, Zeng GS, Utili S, Jiang MJ, Wu L. Analytical solutions of stresses and displacements for deeply buried twin tunnels in viscoelastic rock. Int J Rock Mech Min Sci 2017;1(93):13–29. https://doi.org/10.1016/j.ijrmms.2017.01.002.
[43] Wang Y, Liu J, Guo P, Zhang W, Lin H, Zhao Y, et al. Simplified analytical solutions for tunnel settlement induced by axially loading single pile and pile group. J Eng Mech 2021;147(12):04021116. https://doi.org/10.1061/(ASCE)EM.1943-7889.0002035.
[44] Wu K, Shao Z. Study on the effect of flexible layer on support structures of tunnel excavated in viscoelastic rocks. J Eng Mech 2019;145(10):04019077. https://doi.org/10.1061/(ASCE)EM.1943-7889.0001657.
[45] Wu K, Shao Z, Sharifzadeh M, Chu Z, Qin S. Analytical approach to estimating the influence of shotcrete hardening property on tunnel response. J Eng Mech 2022;148(1):04021127. https://doi.org/10.1061/(ASCE)EM.1943-7889.0002052.
[46] Zaheri M, Ranjbarnia M, Dias D. New analytical approach to simulate the longitudinal fiberglass dowels performance installed at the face of a tunnel embedded in weak and weathered rock masses. Comput Geotech 2023;1(153):105080. https://doi.org/10.1016/j.compgeo.2022.105080.
[47] Zaheri M, Ranjbarnia M, Oreste P. Performance of systematic fully grouted rockbolts and shotcrete layer in circular tunnel under the hydrostatic conditions using 3d finite difference approach. Geomech Geoeng 2021;1(16):198–211. https://doi.org/10.1080/17486025.2019.1648885.
[48] Zou JF, Li C, Wang F. A new procedure for ground response curve (GRC) in strain-softening surrounding rock. Comput Geotech 2017;1(89):81–91. https://doi.org/10.1016/j.compgeo.2017.04.009.
[49] Zhang Q, Wang HY, Jiang YJ, Lu MM, Jiang BS. A numerical large strain solution for circular tunnels excavated in strain-softening rock masses. Comput Geotech 2019;1(114):103142. https://doi.org/10.1016/j.compgeo.2019.103142.
[50] Zhou J, Yang XA, Ma MJ, Li LH. The support load analysis of deep-buried composite lining tunnel in rheological rock mass. Comput Geotech 2021;1(130):103934. https://doi.org/10.1016/j.compgeo.2020.103934.
[51] Zhou S, He C, Guo P, Di H, Xiao J. Three-dimensional analytical model for coupled track-tunnel-soil system in a multilayered half-space. J Eng Mech 2020;146(2):04019121. https://doi.org/10.1016/j.compgeo.2020.103934.